Available online at www.sciencedirect.com
SCIENCE DIRECT®

Journal of the European Ceramic Society 23 (2003) 2047–2052

www.elsevier.com/locate/jeurceramsoc

The application of models for high solids content suspensions to pastes

K.M. Hurysz*, J.K. Cochran

School of Materials Science and Engineering, Georgia Institute of Technology, 771 Ferst Dr. NW, Atlanta, GA 30332-0245, USA

Received 25 June 2002; received in revised form 10 December 2002; accepted 1 January 2003

Abstract

Pastes are a combination of two phases: a solid phase raw material carried by a fluid phase composed of solvent, binder, and additives. Capillary rheometry of the fluid phase followed by capillary rheometry of a paste composition permits calculation of the relative paste bulk shear stress under most circumstances. Non-linear optimization is then used to determine the intrinsic viscosity, $[\eta]$, and maximum solids content, ϕ_{max}, that best satisfy the chosen high solids content suspension model equation. Three criteria were developed that a candidate paste model equation must meet: it must model the experimental data with low error, it must be relatively insensitive to changes in $[\eta]$ and ϕ_{max}, and it must arrive at sensible values for $[\eta]$ and ϕ_{max}. In this investigation, the Mooney, Chong, and Dougherty-Krieger equations were tested. The Dougherty–Krieger equation best met the candidate paste model criteria and was used effectively to model paste properties.

Keywords: Extrusion; Fe_2O_3; Mechanical properties; Modeling; Pastes; Plasticity

1. Introduction

1.1. Extension of fluid phase properties to pastes

Einstein[1] developed a relationship between solids content and the viscosity of an infinitely dilute suspension of rigid spheres. A variety of extensions to this theory have since been presented in the attempt to describe the rheological behavior of higher concentration suspensions. Several of the most commonly used models were proposed by Mooney, Eq. (1); Chong, Eq. (2); and Dougherty and Krieger, Eq. (3).[2–4]

$$\eta_r = \exp\left(\frac{[\eta]\cdot\phi}{1-\frac{\phi}{\phi_{max}}}\right) \tag{1}$$

$$\eta_r = \left[1+\frac{[\eta]\cdot\phi_{max}}{2}\left(\frac{\frac{\phi}{\phi_{max}}}{1-\frac{\phi}{\phi_{max}}}\right)\right]^2 \tag{2}$$

$$\eta_r = \left(1-\frac{\phi}{\phi_{max}}\right)^{-[\eta]\cdot\phi_{max}} \tag{3}$$

Alternative equations presented by Eilers,[5] Maron and Pierce,[6] and Quemada[7] fit the form of the Dougherty–Krieger equation but do not give the highest degree of freedom in describing suspension viscosity.[8]

Equations that model high solids content suspensions consider the solids content, ϕ, the maximum solids content, ϕ_{max}, and an empirically derived hydrodynamic crowding factor, $[\eta]$, known as the intrinsic viscosity. Each model calculates a property value relative to the suspending fluid. The relative viscosity of a suspension, η_r, is defined as the ratio of the suspension viscosity, η_o, to the solvent viscosity, η_s, as shown in Eq. (4).

$$\eta_r = \frac{\eta_o}{\eta_s} \tag{4}$$

Several methods can be used to arrive at an experimental value for ϕ_{max}, whereas $[\eta]$ is a calculated curve fitting parameter. Einstein calculated $[\eta]=2.5$, but positive and negative deviations from this value have been noted experimentally by Jeffrey and Acrivos[9] and Lee et al.[10]

Pastes of the composition used in this investigation have been previously shown to have a response to shear stress and shear rate similar to that of well-dispersed

* Corresponding author.
E-mail address: kevin.hurysz@mse.gatech.edu (K.M. Hurysz).

0955-2219/03/$ - see front matter © 2003 Published by Elsevier Science Ltd.
doi:10.1016/S0955-2219(03)00027-X

suspensions.[11] The similarity suggests that relative viscosity and relative paste bulk shear stress are interchangeable quantities. The exchange is legitimate because the shear stress vs. shear rate curve is analogous to the extrusion pressure vs. extrudate velocity curve. Relative values are unitless so the discrepancy between the units of viscosity and stress are not problematic. The concept of equivalence between suspensions and pastes leads directly to the idea that the models that predict suspension properties at high solids contents can be successfully applied to pastes.

Paste systems behave like particle suspensions because they share many of the same characteristics. Suspensions consist of a homogeneously distributed particulate solid phase carried by a liquid solution.[12] Electrostatic, stearic, van der Waals, or a combination of these forces can result in a stable dispersion. Pastes consist of a mixture of solid phase mechanically separated by a fluid solution.

This study concentrated on the application of high solids content suspension viscosity models to pastes. Non-linear optimization techniques were used to develop contour maps of the error associated with the error associated with the Mooney, Chong, and Dougherty–Krieger equations. The results are the criteria that candidate models must meet to successfully describe paste properties and the model that can be best applied to experimental rheometric data.

1.2. Extrusion

Extrusion is a material forming process that permits the shaping of paste into a linear form that has a constant cross section.[13] The paste is a homogeneous mixture of two phases: a solid phase composed of the particular oxide or oxide mixture carried by a fluid phase of water, binder, and additives.

A novel technology has been developed by Cochran et al.[14,15] for the extrusion of thin walled (<250 μm) ceramic honeycomb and subsequent thermochemical processing of the green structure to metal alloy. The composition used in this investigation is complex because it has been chosen to result in a 350 grade maraging steel following a reduction heat treatment.

Benbow and Bridgewater[16,17] developed an analysis technique using flow through a die of circular cross section to measure the rheological properties of pastes. The model given by Eq. (5) assumes a linear relationship between the extrusion pressure, P and extrudate velocity, V, and has the form:

$$P = 2(\sigma_o + \alpha V)\ln\left(\frac{D_o}{D}\right) + \frac{4L(\tau_o + \beta V)}{D} \quad (5)$$

In this equation, D_o is the diameter of the barrel, D is the diameter of the die land, and L is the length of the die land. Variables σ_o and α are associated with flow into the die land, τ_o and β with flow through the die land. Here, α is a parameter characterizing the effects of velocity on σ_o, τ_o is the die wall shear stress, and β is a parameter characterizing the effects of velocity on τ_o.

2. Experimental procedure

2.1. Paste preparation

The pastes were made by weighing individual components into the appropriate fractions to result in 1500 g batches. Solid raw materials were dry blended for 15 min in a commercial blender fitted with an open mixing paddle. The lubricant was dissolved in water and then added to the powder–binder blend. Mixing continued for 2 min following the fluid addition. The granulated powder was pugged in a Buss kneader for approximately 5 min.

2.2. Measurement of maximum solids loading

The oil drop test is a modification of the ASTM standard Gardner-Coleman (D 1483-95) and spatula rub-out (D 281-95) tests and is used to rapidly estimate ϕ_{max}. In the oil drop test, approximately 40 g of dry mixed powder raw material was mixed with corn oil by hand in a small plastic bag. Use of oil reduces evaporation and provides good wetting of the powder. The liquid fraction is increased dropwise until a cohesive, workable paste having smooth texture and shape-retaining character is formed.[17] Maximum solids content is then calculated from the weight of oil needed for pore saturation, the powder weight, and respective densities. This method provides a means to measure the fluid content needed to fill interparticle voids under mildly sheared conditions.

The reciprocal bulk shear stress test involves a linear extrapolation of the reciprocal of extrusion pressure against the ratio of fluid volume (V_f) to solid volume (V_s). The value of V_s at 0 MPa^{-1} represents the critical value where the liquid phase exactly fills interparticle voids. Compositions to the left of this critical value cannot be extruded because particles interlock and there is no mechanism to facilitate fluid flow. Any composition to the right of the intercept represents excess fluid and is theoretically extrudable. The resistance of a paste to a deforming stress is highly dependent on the thickness and rheology of the fluid layer that surrounds the particles. The thickness of this layer is directly proportional to the excess of liquid phase above that required to fill particle interstices.

2.3. Capillary rheometry

Extrusion testing was conducted using a custom, stainless steel piston extruder fitted to a Satec test frame. A schematic of the testing device is shown in

Fig. 1. Seay[18] established that wall stresses between the paste and the barrel were small enough to be ignored.

The extrusion pressures at several speeds were measured with a single barrel of paste. The barrel was charged with paste to a depth of 100 mm and tamped to remove large air pockets. The piston was inserted into the barrel and driven downward by the test frame at each of six constant extrudate velocities: 68.5, 27.4, 13.7, 6.9, 2.7, and 1.4 mm/s. Testing proceeded from fastest to slowest, followed by a return to the fastest velocity. Repeat measurements at the fastest velocity did not deviate from each other by more than 10% and no corrections were applied to results. Statistical analysis of error in property measurements was not undertaken because of the length of time required to prepare and characterize each sample.

The data obtained for each paste are the ram force at each velocity for each die. Three interchangeable dies of circular cross section, 3.18 mm diameter, and L/D ratios of 1, 8, and 16 are fitted to the rheometer. Extrapolating a plot of L/D ratio against P to zero enables the calculation of bulk shear stress.

Six pastes of 350 grade maraging steel composition and varying solids fractions were prepared with a constant water to binder weight ratio of 4:1 and a constant lubricant concentration of 0.5% of the powder weight. The solids contents tested were 0, 30, 40, 50, 55, and 60 vol.%. The test at 0 vol.% solids (the fluid phase) permits calculation of relative properties.

2.4. Material

A4M Methocel, a moderate molecular weight methylcellulose from Dow Chemical was used as a binder. Pegosperse 100S, an ethoxylated stearic acid from Lonza was used in small concentrations as a lubricant. These additives are observed to burn out cleanly through chemical reaction or reduction during heat treating. Distilled, deionized water was used as a solvent in all experiments.

A mixture of oxides that when reduced forms 350 grade maraging steel was used as the solid phase. A series of identically prepared pastes were formulated having the batch composition described in Table 1.

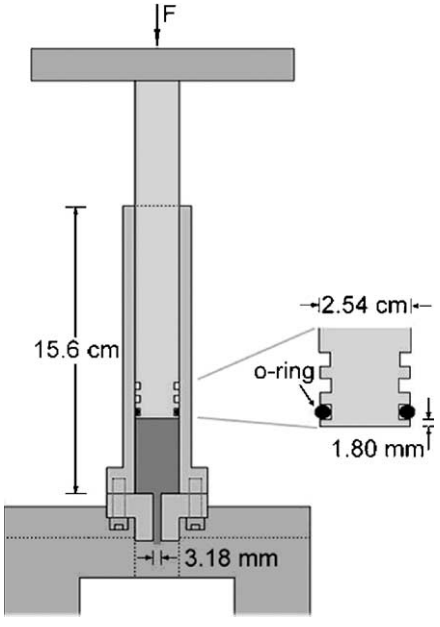

Fig. 1. Schematic of the capillary rheometer. Inset: head of ram.

3. Results and discussion

3.1. Properties of the paste

Raw materials were characterized via Scanning Electron Microscopy (SEM) imaging, particle size analysis, and BET surface area and pore volume analyses. SEM imaging revealed a generally equiaxed particle structure, with the exception of Mo, which had a residual sponge morphology. Particle size ranged from approximately 1–12 μm, with an average size near 6 μm. Particle surface area ranged from 0.4 to 4.0 m^2/g. Desorption hysteresis indicated internal porosity of the raw material powder at 3.1%. A characterization summary is shown in Table 1.

The data from each set of paste experiments are plotted on a graph of die length to diameter ratio against extrusion pressure. From Eq. (5), as L/D approaches 0,

$$P = 2(\sigma_o + \alpha V)\ln(D_o/D) \quad (6)$$

Fig. 2 is a summary of the extrapolations of L/D to 0 for each extrudate velocity and paste composition. The measured bulk shear stress at each solids content is given in Table 2. Increasing the solids content results in exponential increases in extrusion pressure. Extrusion

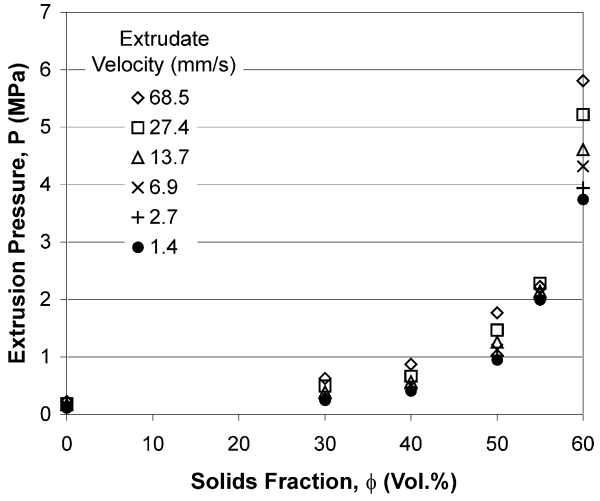

Fig. 2. Summary of the extrapolations of L/D to 0 for each extrudate velocity and paste composition.

Table 1
Characterization and batch composition of 350 grade maraging steel pastes

	Source	Particle size (μm) at CWPF than			BET surface (m^2/g)	Pore volume (%)	
		10%	50%	90%			
Raw material							*Amount in batch* (%)
Fe_2O_3	Pea ridge iron ore	0.8	4.5	10.0	1.51	2.4	66.7
NiO	Ceramic color	3.3	6.3	11.8	0.48	1.8	16.7
Co_3O_4	Ceramic color	3.0	3.7	4.5	4.04	8.7	11.9
Mo	Atlantic equipment	2.7	7.0	15.6	0.54	2.8	3.5
TiH_2	Reading alloys	2.0	6.8	15.4	0.48	1.0	1.1
Fluid material							*Amount in fluid* (%)
A4M Methocel	Dow Chemical Co.						19.6
100S Pegosperse	Lonza						2.0
H_2O							Balance

Table 2
Values of ϕ_{max} and $[\eta]$ resulting in minimum error

Equation	ϕ_{max} (vol.%)	$[\eta]$
Dougherty–Krieger	67	2.3
Chong	70	2.4
Mooney	85	1.7

pressure is especially sensitive to solids content as ϕ approaches ϕ_{max}. Higher solids content results in an increased frequency of particle–particle and particle–surface interactions. The dimensionally thinner fluid phase separating and lubricating the particles translates directly to rapid increases in paste bulk shear stress.

Each of the pastes tested showed a distinct yield point and a near linear pressure increase with a corresponding increase in velocity. As ϕ approaches ϕ_{max}, behavior becomes increasingly pseudoplastic (shear thinning) as shown in Fig. 3. This transition suggests that measurements will be prone to error as ϕ_{max} is approached because the requirements of the model are not being met.

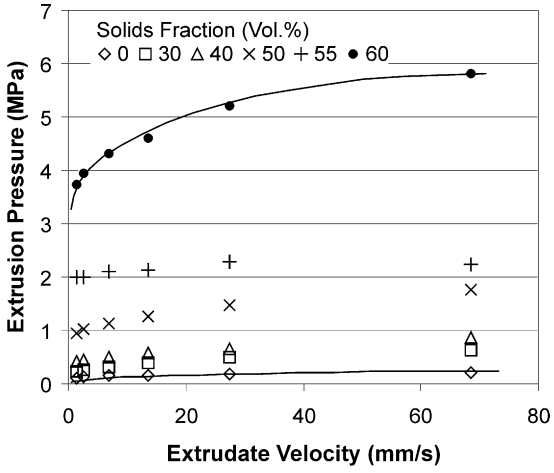

Fig. 3. Crossplot of extrudate velocity against extrusion pressure for each paste composition.

3.2. Determination of maximum solids loading

The utility of the oil drop test arises from the fact that a single, small sample can be used to determine the maximum solids loading without the difficulty of extensive processing and rheometric investigation. The direct result of the oil drop test without correction is that $\phi_{max} = 59.6$ vol.%.

The oil drop test tends to underestimate ϕ_{max} because hand mixing is a low shear operation and can be ineffective in breaking up agglomerates. The amount of liquid present at ϕ_{max} has been historically assumed to be 90% of the oil drop test value.[17] By applying this criterion to the test results, ϕ_{max} was estimated to be 62.1 vol.%. By plotting the reciprocal of the paste bulk shear stress against the ratio of fluid to solid volume for the six pastes, as shown in Fig. 4, ϕ_{max} was measured to be 64.2 vol.%.

3.3. Application of suspension models to pastes

For each of Eqs. (1)–(3), σ_o was substituted for η_o. Non-linear optimization was used to determine the pair of ϕ_{max} and $[\eta]$ values that best fit each model equation. For each paste solids content, a matrix was developed that consisted of values of $[\eta]$ between 0.5 and 4.0 and values of ϕ_{max} between 60 and 85 vol.%.

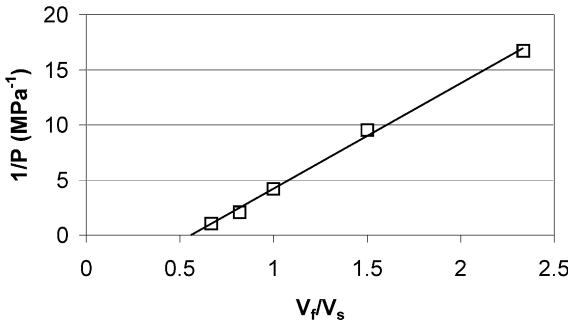

Fig. 4. Determination of ϕ_{max} from measurements of paste bulk shear stress.

The Mooney, Chong, and Dougherty–Krieger equations were then solved for each pair of values, as dictated by the matrix. Values of ϕ are fixed by paste composition, and σ_o is measured experimentally via capillary rheometry. Error was then calculated using the χ^2 method.

The error functions are plotted in contour for the Mooney, Chong, and Dougherty–Krieger equations in Fig. 5a, b, and c, respectively. The values on the contour plots represent χ^2 error. As there is no method available to directly measure $[\eta]$, agreement of calculated ϕ_{max} values with independently determined, experimental values becomes the critical variable in choosing a model to describe paste behavior.

There are three specific criteria that a candidate model equation must meet: (1) it must model the experimental data with low error; (2) it must be relatively insensitive to changes in $[\eta]$ and ϕ_{max}; and (3) it must arrive at sensible values for $[\eta]$ and ϕ_{max}. Each equation in this investigation fits the data with a shallow error function. The minimum error is substantially the same for the ideal solution of each equation ($\chi^2 \sim 0.4$). The combination of $[\eta]$ and ϕ_{max} that result in the minimum error from the analysis of each equation is presented in Table 2. It is thus the breadth of the error trough and the legitimacy of the minimum error solution that in this case establish the best model equation.

The error in fitting the Mooney equation is minimized at $[\eta] = 1.7$ and $\phi_{max} = 85$ vol.%. This high value for ϕ_{max} is not consistent with particle packing theory or the values of ϕ_{max} determined independently.[19] Of the models tested, the Mooney equation is moderately insensitive to changes in $[\eta]$ and ϕ_{max}.

The error in fitting the Chong equation is minimized at $[\eta] = 2.4$ and $\phi_{max} = 70$ vol.%. While the values for both ϕ_{max} and $[\eta]$ are reasonable, the error function is much more steep and narrow than the other candidate models. As a result, small changes in $[\eta]$ and ϕ_{max} cause large increases in error.

The error in fitting the Dougherty–Krieger equation is minimized at $[\eta] = 2.3$ and $\phi_{max} = 67$ vol.%. Values of ϕ_{max} between 64 and 68 vol.% and values of $[\eta]$ between 1.9 and 2.3 bound the lowest error region of the plot. The theoretical value of ϕ_{max} calculated by the Dougherty–Krieger equation agrees most closely with the values determined experimentally. A comparison of an equivalent change in $[\eta]$ and ϕ_{max} across each of the models tested results in the smallest increases in error with the Dougherty–Krieger equation.

At the value of ϕ_{max} obtained via the reciprocal bulk shear stress method, 64.2 vol.%, the lowest error $[\eta]$ calculated from the Dougherty–Krieger equation, is 2.0. At the value of ϕ_{max} obtained via the oil drop test, 62.1 vol.%, the Dougherty–Krieger equation still provides the best fit. The error for this case is necessarily larger because of the larger difference between calculated and experimental ϕ_{max}.

Fig. 6 shows the relative bulk shear stress of the pastes and a plot of the Dougherty–Krieger equation at the overall minimum error combination from non-linear regression, $\phi_{max} = 67$ vol.% and $[\eta] = 2.3$. This plot compares favorably with the minimum error combination from the reciprocal bulk shear stress method, $\phi_{max} = 64.2$ vol.% and $[\eta] = 2.0$. When the oil drop test value is used for ϕ_{max} and Einstein's value is used for $[\eta]$, deviation from the experimental data is observed, especially at high ϕ.

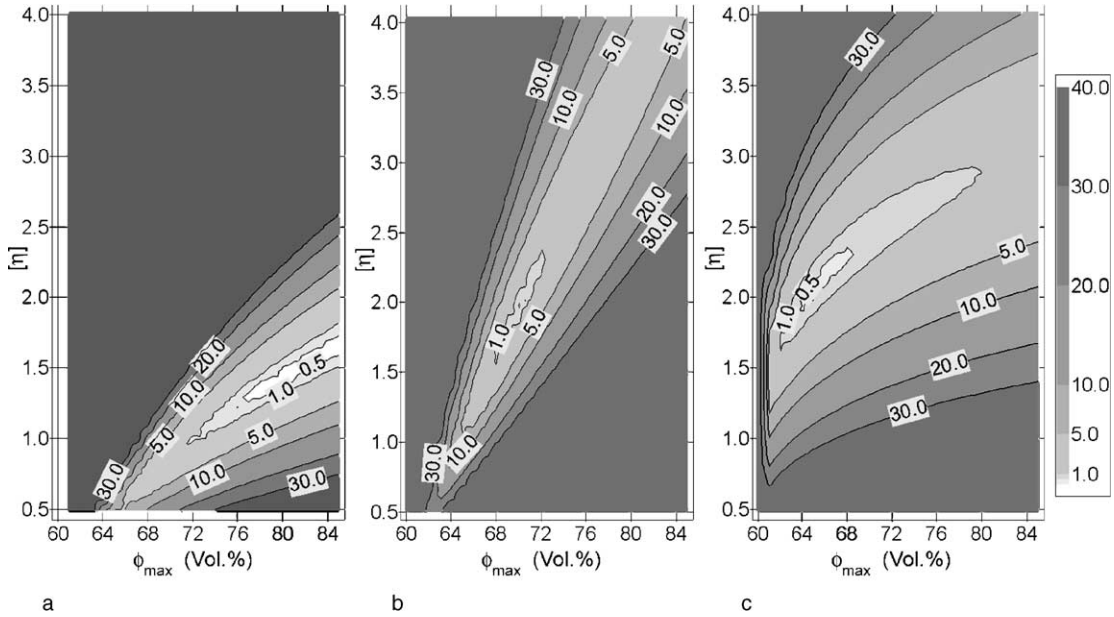

Fig. 5. Contour plots of χ^2 error for the (a) Mooney, (b) Chong, and (c) Dougherty–Krieger equations.

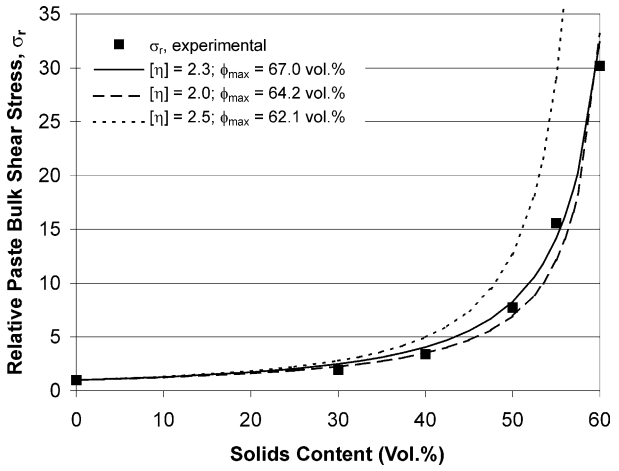

Fig. 6. Experimental relative bulk shear stress of the 350 grade maraging steel pastes compared to plots of the Dougherty–Krieger equation at a variety of ϕ_{max} and $[\eta]$ combinations.

4. Conclusions

Non-linear optimization of candidate high viscosity suspension models determined the pair of $[\eta]$ and ϕ_{max} values that best fit experimental capillary rheometry data. For each model equation, σ_o was substituted for η_o. Of the Mooney, Chong, and Dougherty–Krieger equations, the Dougherty–Krieger equation best meets the criteria for a candidate paste modeling equation. It fits the experimental data with low error, is relatively insensitive to small changes in $[\eta]$ and ϕ_{max}, and arrives at sensible values for $[\eta]$ and ϕ_{max}.

The oil drop test estimates ϕ_{max} to be 62.1 vol.%. A plot of $1/P$ against the ratio of fluid volume to solid volume is approximately linear. The value of V_s at the x-intercept represents the maximum solids loading, 64.2 vol.%. At both of these ϕ_{max} values, the Dougherty–Krieger equation outperformed the Mooney and Chong equations for the modeling of paste properties.

Acknowledgements

This work was sponsored by DSO of DARPA (N00014-99-1-1016) under Dr. Leo Christodoulou and by ONR (N0014-99-1-0852) under Dr. Steven Fishman.

References

1. Einstein, A., Eine neue Bestimmung der Molekuldimensionen. *Ann. Phys*, 1906, **19**, 289–306 (English translation in Einstein, A., *Investigation on the Theory of Brownian Motion*. Dover, New York, 1956).
2. Mooney, M., The viscosity of a concentrated suspension of spherical particles. *J. Colloid Sci.*, 1957, **6**, 162–170.
3. Chong, J. S., Christiansen, E. B. and Baer, A. D., Rheology of concentrated suspensions. *J. Appl. Poly. Sci.*, 1971, **15**, 2007–2021.
4. Krieger, I. M. and Dougherty, T. J., A mechanism for non-Newtonian flow in suspensions of rigid spheres. *Trans. Soc. Rheol*, 1959, **3**, 137–152.
5. Eilers, H., Die viskosität von emulsionen hochviskoser stoffe als function der konzentration. *Kolloid Z*, 1941, **97**, 313–321.
6. Maron, S. H. and Pierce, P. E., Application of Ree-Eyring generalized flow theory to suspensions of spherical particles. *J. Colloid Sci.*, 1956, **11**, 80–95.
7. Quemada, D., Rheology of concentrated disperse systems. *Rheol. Acta*, 1978, **17**, 643–653.
8. Windhab, E. J., Fluid immobilization—a structure-related key mechanism for the viscous flow behavior of concentrated suspension systems. *Appl. Rheol*, 2000, **10**(3), 134–144.
9. Jeffrey, D. J. and Acrivos, A., The rheological properties of suspensions of rigid particles. *A. I. Chem. E. J, 1976, 417–422.*
10. Lee, J., So, J. and Yang, S., Rheological behavior and stability of concentrated silica suspensions. *J. Rheol*, 1999, **43**(5), 1117–1141.
11. Hurysz, K. M., *Paste Mechanics for Fine Extrusion*. PhD Dissertation, Georgia Institute of Technology, Atlanta, GA, 2001.
12. Cesarano, J. and Aksay, I. A., Processing of highly concentrated aqueous alpha-alumina suspensions stabilized with polyelectrolytes. *J. Am. Ceram. Soc.*, 1988, **71**(12), 1062–1067.
13. Reed, J. S., *Introduction to the Principles of Ceramic Processing*. Wiley, New York, 1988.
14. Cochran, J. K., Lee, K. J., McDowell, D. and Sanders, Jr., T., Multifunctional metallic honeycombs by thermal chemical processing. In *Processing and Properties of Lightweight Cellular Metals and Structures*, TMS, Warrendale, PA, 2002, pp. 127–136.
15. Hurysz, K. M., Oh, R., Cochran, J. K., Sanders, Jr., T. H. and Lee, K. J., Modeling powder extrusion pastes for forming light weight multifunctional structures. In *Processing and Properties of Lightweight Cellular Metals and Structures*, TMS, Warrendale, PA, 2002, pp. 167–176.
16. Benbow, J. J., Oxley, E. W. and Bridgwater, J., The extrusion mechanics of pastes—the influence of paste formulation on extrusion parameters. *Chem. Eng. Sci.*, 1987, **42**, 2151–2162.
17. Benbow, J. and Bridgwater, J., *Paste Flow and Extrusion*. Clarendon, Oxford, UK, 1993.
18. Seay, W. D., *Capillary Rheometry Evaluation of Honeycomb Extrusion Pastes*. Master's Thesis, Georgia Institute of Technology, Atlanta, GA, 2001.
19. Dinger, D. R. and Funk, J. E., Particle-packing phenomena and their application for materials processing. *MRS Bulletin*, 1997, **22**(12), 19–23.